

Performance evaluation of bubble column photobioreactor along with CFD simulations for microalgal cultivation using human urine

Sanjeet S. Patil^a, Bunushree Behera^b, Sujit Sen^a, P. Balasubramanian^{b,*}

^a Department of Chemical Engineering, National Institute of Technology Rourkela, 769 008, India

^b Agricultural & Environmental Biotechnology Group, Department of Biotechnology & Medical Engineering, National Institute of Technology Rourkela, 769 008, India

ARTICLE INFO

Editor: G. Palmisano

Keywords:

Microalgae
Computational fluid dynamics
Growth kinetics
Human urine
Photobioreactors

ABSTRACT

Optimization of microalgae cultivation to reduce the associated costs is one of the major objectives in a bio-refinery model. The present study optimized the microalgal cultivation using 4.5–8.5 % v/v of DHU (diluted human urine) as a cost-effective resource, in a bubble column photobioreactor (BCPBR) under real-time conditions. Media with 5.5 % DHU and 4% CO₂ showed maximal biomass productivity of 0.14 g L⁻¹ day⁻¹ with a final concentration of 1.06 g L⁻¹. Phosphate and ammonium removal of 90.70 % and 84.10 % respectively was achieved. The biofixation of CO₂ obtained for 6 days, during the cultivation in 5.5 % DHU, by supplying 4% of CO₂ enriched air was 0.29 g L⁻¹ d⁻¹. Computational fluid dynamics (CFD) simulations were used to study the effects of velocity magnitude, shear stress, turbulent kinetic energy, and irradiance on the microalgal growth inside the BCPBR. The developed kinetic model predicted the biomass concentration and phosphate removal up to 98 % and 82 % accuracy respectively. Such studies would aid in comprehending the large scale commercial cultivation and thereby facilitate the application of microalgae in the future.

1. Introduction

The global carbon emissions are rising at an unprecedented rate, the effects of which are clearly visible in the drastic climate change taking place over the last decade [1]. Therefore, to combat these repercussions a steep reduction in carbon dioxide (CO₂) levels must be given a high priority. Further, utilizing those captured CO₂ to synthesize bioenergy would complement the energy sector in addition to combating environmental concerns. Amongst all, biofuel from microalgae seems the most potent resource for clean energy production. The CO₂ sequestration efficiency of microalgae is 10–50 times more than terrestrial plants [2]. The high lipid yield and ability to cultivate on non-arable land gives it an advantage over the biofuel produced from food crops. Wastewater remediation by the cultivation of microalgae is more attractive compared to chemical treatment as it efficiently and economically removes the nutrients and contaminants from wastewater [3].

Source separated human urine can provide enough nutrients for large scale microalgal growth thereby could act as a cost-effective way of reducing the nutrient load of municipal wastewater treatment plants [4]. Previous studies on microalgal growth using human urine as a nutrient source have been done in a controlled environment [5] and on a

lab-scale having small culture volume [3,6]. Since it is difficult to anticipate the actual outcome from laboratory studies having a very controlled environment for biomass growth and nutrient recovery, conducting studies in outdoor conditions under a real time scale is necessary.

Most of the outdoor scale studies are usually carried out in raceway ponds rather than photobioreactor [PBR] [7]. Open ponds are economical and durable but are subject to evaporative losses and contamination from various organisms. Among various PBRs, bubble column PBR (BCPBR) is comparatively easy to design and construct, and it provides excellent mass and heat transfer characteristics while consuming less floor space [8]. Production of individual-specific algal strains is more feasible in BCPBR than open ponds, as they are less prone to contamination, provide better control over the process conditions and efficient CO₂ utilization [1]. The disadvantage of light penetration in dense culture can be resolved with improved mixing and by providing internal illumination [4]. Microalgae cultivation in BCPBR can provide an effective way of sequestering CO₂ from flue gas and treating source separated wastewater simultaneously [9].

Many researchers like Hsueh et al., [10]; Xin et al., [11] owing to their simplicity have utilized a single nutrient factor (N, P, CO₂) to

* Corresponding author.

E-mail address: biobala@nitrkl.ac.in (B. P.).

model algal growth kinetics in wastewater. Multinutrient model employing light and CO₂ concentration had been utilized by **Pegallapati and Nirmalakhandan**, [12] modelled the growth of *Nannochloropsis sp.*, and *Scenedesmus sp.*, considering the light, nitrogen and CO₂ effects in semicontinuously operated bubble column PBR. The microalgal kinetic growth model of *Desmodesmus sp.*, and *S. obliquus* was done by **Eze et al.**, [13] considering N, P, and CO₂ multifactor co-limitation effects. **Lee et al.**, [14] and **Darvehei et al.**, [15] have enlisted the pros and cons of different kinetic models for algal growth.

Flow hydrodynamics play an essential role in governing the performance in photobioreactors [16]. According to previous researchers, the performance of reactors was mostly estimated based on overall reactor volume considering average irradiance and perfect mixing [17]. However, owing to sedimentation and light attenuation most outdoor scale PBRs are operated under imperfect mixing conditions. Therefore, it is essential to simulate the performance of PBRs via integrating the computational fluid dynamics. **Nauha and Alopaeus**, [18] utilized an integrated compartmental fluid flow model in association with the growth model based on the concept of the photosynthetic algal factory, and postulated that the movement of algal cells in the reactor allows the continued growth of microalgae, even at high biomass concentration when light is limited only near the walls of the BCPBRs. The compartmentalized model was further improvised with the inclusion of directionality of light and night loss to predict the mass transfer, system hydrodynamics, and the algal growth rate in BCPBRs accurately [19]. **Hadiyanto et al.**, [20] used CFD to simulate the hydrodynamics based on the design characteristics of high rate algal ponds and predicted a length to width ratio of more than 10 is necessary to provide better mass transfer for efficient reactor performance. A sliding mesh CFD model has been used by **Hreiz et al.**, [21] to predict the flow velocity and mixing time inside the open PBR. The multiphysics approach based on Lagrangian and Eulerian methods has been utilized for simulating the algal growth kinetics inside PBRs. A recent study by **Gao et al.**, [22] for predicting the growth rate of algae in airlift PBR showed that shear stress often inhibits the photosynthetic activity of microalgae and also the Eulerian approach provides better estimates compared to the Lagrangian approach. The eulerian approach showed appropriate goodness of fit during the simulation of algal growth in Taylor vortex PBR [23]. **Gao et al.**, [16] have reviewed the merits and issues associated with different computational models for assessing the predictive modelling during reactor design and scale-up. Lagrangian approach assumes non-uniform distribution of cells in the annular region due to unphysical trapping and unavailability of grid resolution, while the Eulerian approach assumes uniform distribution of algal cells in the annular region [24]. Eulerian approach is computationally more efficient than Langragian method and the predictive model can be easily extended to large reactors without the need to further generate large notion/particle history trajectories [16]. The study by **Gao et al.**, [23] have reported that the simulation approach though could be efficiently applied to reactors with moderate microalgal biomass concentration, often an increase in biomass content requires grid refinement to avoid improper resolution issues associated with the velocity field.

Common computational approaches to simulate the flow or dispersion of bubbles in a continuous liquid medium includes different methods like Volume-of-fluid (VOF), Eul Eulerian-Lagrangian, and Eulerian–Eulerian. VOF method is regarded to be well-suited for a single fluid-fluid interface and has been used along with fluid volume fraction transport and momentum balance equation for simulations in raceway ponds [21,25]. However, the sensitivity of prediction in this approach reduces with increase in number of gas bubbles. Eulerian–Lagrangian approach assumes the continuous liquid phase as a continuum and computes trajectories of notional bubbles utilizing a force balance equation. Researchers like **Olivieri et al.**, [26] and **Huang et al.**, [27] utilized these approach to evaluate the gas-liquid flow in PBRs, with an advantage of tracking numerous point-mass bubbles as individual bubble surfaces are not resolved. The disadvantage of these methods lies

with the high computational costs, that restricts its use to small scale reactors. The Eulerian–Eulerian approach treats gas and liquid phases as interpenetrating continua, and utilizes different momentum and continuity equations to solve them. This method is widely used being computationally more efficient because of the lack of requisition to resolve gas-liquid trajectories or the need to track individual trajectories [16].

The review by **Lee et al.**, [14] and **Darvehei et al.**, [15] have summarized the different single factor and multifactor based microalgal kinetic models and have proposed that most of them are restricted to the utilization of factors like N, P, CO₂ and pH. Modelling studies with respect to outdoor scale cultivation is very limited, as large scale algal cultivation is often influenced by the solar intensity and temperature along with the presence of multiple algal species, rather than a single axenic culture. Thus, robust model must incorporate temporal variations in sunlight and temperature along with the conditions prevailing in freshwater ecosystem. Also, extensive study with the integration of computational fluid dynamics (CFD) along with algal growth in BCPBRs using diluted human urine is still lacking.

The present study aimed to examine the adaptability and productivity of a native microalgal consortium under uncontrolled and real-time conditions using diluted human urine to minimize the cost of cultivation. The efficiency of a 7 L working volume bubble column PBR, with various dilution of human urine (21.22X, 17.18X, 14.38X, 10.76X) [4.5–8.5 % (v/v)] were evaluated for determining the algal biomass concentration and nutrient removal efficiency. The difference in effect on algal growth by feeding CO₂ from atmospheric air and 4% v/v CO₂ enriched air was also observed. To study the hydrodynamics inside the BCPBR, CFD simulations were used for comprehending the efficiency of mixing, velocity contours, the amount of turbulent kinetic energy and irradiance at different temporal and spatial conditions. A robust, and flexible growth kinetic model was used with phosphorus as limiting nutrient along with the temporal variations, which can be applied to any geometry of PBRs to simulate the biomass growth and nutrient uptake using user-defined functions in Ansys Fluent v15. To the best of author's knowledge, this is the first study with CFD for predicting the growth rate of microalgae in a BCPBR with the use of diluted human urine as nutrient media. Results obtained through CFD simulations were validated with the data obtained in experimental outdoor scale cultivation. Such studies would aid in designing PBRs for large scale cultivation of microalgae, before proceeding for costly and time-consuming field trials.

2. Materials and methods

2.1. Microalgal inoculum

Mixed microalgal consortium from the National Institute of Technology (NIT) Rourkela (India) open ponds was collected. Initially, the culture was maintained in synthetic BG11 media with artificial white fluorescent lights (36 W, 0.44 A) at ambient air temperature (30 ± 5 °C). To reduce the cost factor involved during cultivation, the mixed algal consortium was later enriched and grown with diluted human urine (6.5 % v/v) under optimized conditions in autotrophic mode resulting in a specific growth rate of 0.26 d⁻¹ [6]. As microscopically examined, the microalgal consortium mainly dominated by *Chlorella sp.*, along with *Spirulina sp.*, *Scenedesmus sp.*, and *Synechocystis sp.*, was used as an inoculum for reactor studies [28]. The undiluted human urine was light yellowish in colour with a pH of 6.5 ± 0.3, having 4.6 ± 0.35 mg/mL ammonium, 0.26 ± 0.1 mg/mL phosphate measured by standard methods for the examination of water and wastewater as detailed in **Behera et al.**, [6]. 0.19 ± 0.09 mg/mL sodium, 1.65 ± 0.31 mg/mL potassium and 0.63 ± 0.17 mg/mL calcium, was obtained by using a microprocessor-based flame photometer (model 1385) calibrated with the appropriate standards. No glucose presence was detected by dinitrosalicylic acid (DNS) method [29]. The microalgal species have been

well-acclimatized by repeated subculturing over two years in diluted human urine, to avoid any variation in growth or algal community due to batch variation of nutrients in urine.

2.2. Photobioreactor design and operating conditions

A cylindrical BCPBR of length 63 cm and inner diameter of 14 cm made out of plexi-glass was constructed. The bubble column had a working volume of 7 L. The cultivation system comprised of a BCPBR, CO₂ gas cylinder, an air pump, three rotameters to control the flow of air, CO₂ and mixture of CO₂ and air, spherical air stone sparger of 2 cm diameter to feed in the required gas. The PBR was covered on top with a disc having three holes, each of 8 mm diameter to allow sampling and for sparging air inside the reactor. During the experiments, the airflow rate was maintained at 1.2 L min⁻¹ while the CO₂ flow rate was maintained at 0.04 L min⁻¹ with the help of rotameter. The flow rate of air and CO₂ mixture, after accounting for the head losses, was maintained at 1 L min⁻¹. Likewise, the flow rate was optimized to provide a 4% CO₂ enriched air inside the PBR through the air stone sparger. Razzak et al., [30] cultivated *Chlorella vulgaris* in a vertical tubular reactor by supplying CO₂ in varied concentrations i.e. from 2 %–12 % (v/v) and concluded that 4% CO₂ enriched air provided the maximum biomass growth. Sydney et al., [31] have stated the concentration from 2 %–5 % (v/v) of CO₂ enriched air is considered optimal for the growth of *Chlorella vulgaris*. Since, the microalgal consortium mainly consisted of *Chlorella sp.*, to provide optimal conditions for biomass growth, 4% (v/v) of CO₂ enriched air was supplied in the current study. Prior to cultivation with enriched CO₂ air, experiments were conducted with atmospheric air during which the flow rate of 1 L min⁻¹ at an ambient temperature of 27 ± 5 °C and 57 bar pressure was maintained. The flow rate was maintained at 0.14 vvm (below 0.19 vvm) to avoid the effects of shear stresses on microalgal growth [32].

2.3. Experimental procedure

The BCPBR was inoculated with 500 mL of 0.07–0.15 g L⁻¹ concentration of microalgae in 7 L of working volume every time for each of the experiment. The microalgal consortium was grown with DHU of varying concentrations 4.5 %–8.5 % v/v, over a period of 6 days under ambient air conditions at 30 ± 5 °C. The concentration of diluted human urine (DHU) [4.5 %–8.5 %] (v/v) was selected, since the algal consortium was found to grow best at the concentration below 10 % (v/v) of urine. Through a multivariable optimization using response surface methodology, authors have earlier reported highest biomass and lipid productivity for the same algal consortium using 6.5 % (v/v) of diluted urine under autotrophic mode at lab scale [6]. To extrapolate the results from controlled environmental conditions in lab to outdoor scale, studies were carried out using varying concentrations of diluted human urine supplemented with 4% (v/v) of CO₂ enriched air. 6 days were chosen since from the preliminary studies it has been established by the authors that until 6th day the culture remains in the exponential phase. At the end of the exponential phase, the biomass was harvested for use as bio-fertilizers and conversion into biofuel. The experiments were conducted, under real-time conditions in September – December, thus the average ambient air temperature average was at 27 ± 5 °C.

Sampling of the culture was done every 24 h in 15 mL falcon tubes for different analysis. The biomass concentration and nutrient uptake rate were measured spectrophotometrically as detailed by Behera et al., [6]. The supernatant after centrifugation was tested for the presence of ammonium and phosphate ions using standard methods for the examination of water and wastewater as mentioned in Behera et al., [6].

The percentage (mass fractions) of carbon, nitrogen, sulphur and hydrogen in the dried algal biomass was estimated using CHNS elemental analyser and the biofixation of CO₂ or the CO₂ uptake rate (g L⁻¹ d⁻¹) by the microalgae was measured using Eq. (1) [33].

$$CO_2 \text{ uptake rate} = \frac{(X_t - X_o)}{t} \times \frac{C_f}{V} \times \frac{M_{CO_2}}{M_C} \quad (1)$$

Where X_t and X_o are final and initial biomass concentration respectively in g L⁻¹, while the terms C_f, M_{CO₂} and M_C represents the mass fraction of carbon in dried biomass (%), molar mass of CO₂ (g mol⁻¹) and molar mass of carbon (g mol⁻¹) respectively. The terms V and t represents the volume of the reactor in L and the time period of cultivation in days respectively.

2.4. Computational fluid dynamics

CFD was used to simulate the hydrodynamics inside the BCPBR. Eulerian multiphase model with primary phase as water and secondary as air was used. The stokes number of microalgae being less, it was not considered as a distinct phase. The Euler-Euler approach applied in these simulations treats different phases as interpenetrating continua (**Ansys Workbench Help 15**). The biological kinetics of microalgae were integrated with the physical model by applying user-defined functions. The simulations were carried out in Ansys Fluent v15.

2.4.1. Fluid flow model

The 2-D planar geometry of the BCPBR was constructed using the ANSYS software. The relevance center was set as coarse, to reduce the computational load while face size and maximum element size were set as 0.001 m. The grid independence was checked with various combinations of nodes and elements. Some of the combinations of nodes and elements used were [68560, 67900], [57758, 57152], [88771, 87972] and [102655, 101845]. Out of these the combination of 88771 nodes and 87972 proved to give accurate results with lesser computational cost. This provided a minimum orthogonal quality of 0.8314 (orthogonal quality ranges from 0 to 1, where values close to 0 corresponded to low quality) (**Ansys Workbench Help 15**). Transient simulations with pressure-based solver were employed having 2D planar space. The gravity was set to -9.8 m s⁻² in Y-direction. The eulerian multiphase model was applied with 2 phases where the primary phase was chosen as water and the secondary phase was set as air. The algal cells have very small Stokes number so there was no necessity of having a separate phase [22]. The growth model of algae was incorporated through user-defined functions. Standard k-epsilon model was chosen for turbulence modeling. The drag forces and non-drag forces like lift force and wall lubrication force were modeled using the Grace model, Tomiyama model, and Antal-et-al model respectively [34]. The air stone sparger was used for volume flow inlet with 1.2 L min⁻¹ of airflow (volume fraction 1) at an ambient temperature of 27 ± 5 °C and 57 bar pressure. Interior surface (body walls) of PBR were given no-slip boundary condition. The top of PBR was set at degassing boundary conditions. Phase coupled SIMPLE model was used for pressure velocity coupling; the least square-based model was used for obtaining the gradient and, the first-order upwind model for calculating the turbulent kinetic energy and turbulent dissipation rate. Transient simulations were done with a fixed time step of 1 s and maximum iterations per time step were set at 20. Time step 1 s and 20 iterations per time step were chosen as it provided satisfactory results and lesser computation load, based on the time step sensitivity analysis previously done by authors with the range of 10⁻² s to 1 s.

2.4.2. Growth kinetics model

The growth kinetic model was built out of differential equations derived from mass balance done based on the process of biomass growth and nutrient uptake. A robust model was applied in the present study which can be integrated easily with the geometry of any available PBR. A similar model has been used in the simulation of *Nanochloropsis sp.* cultivation in the raceway pond by Park, [35]. Each element of the geometry has been treated as a chemostat with variable inflow and

outflow.

The mass balance equation for algal biomass (X) in the photobioreactor has been represented in Eq. (2)

$$\frac{dX}{dt} = \mu \left(\frac{C}{C + K_C} \right) \left(\frac{P}{P + K_P} \right) \left(\frac{I}{I + K_I} \right) g(T) X - DX \quad (2)$$

Where, the change of algal biomass concentration with time is given by $\left(\frac{dx}{dt}\right)$, X, C and P represents the instantaneous biomass, carbon dioxide and phosphate concentration in g L^{-1} respectively. I is the instantaneous light irradiance in W m^{-2} . K_C , K_P represents half-saturation constants of CO_2 and phosphate in g L^{-1} and, and K_I represents the half-saturation constant for light irradiance in W m^{-2} . μ represents the specific growth rate and D represents the death coefficient both with unit as day^{-1} .

$g(T)$ represents the effect of temperature that has been considered by the assumption of exponential variation of the non-optimal temperature using Eq. (3) [36].

$$g(T) = e^{-m(T-T_{opt})^2} \quad (3)$$

Where, the terms T and T_{opt} represents the water temperature and the optimum water temperature required for algal growth in K, m is the empirical constant for non-optimal temperature in K^{-2} .

The mass balance equation for carbon, in terms of convective mass transfer of CO_2 involving gas flux and diffusion of CO_2 in the liquid phase has been provided in Eq. (4).

$$\frac{dC}{dt} = \frac{F}{V} (C_o - C) + k_L a (C^* - C) - \mu X Y_{C/X} \quad (4)$$

$\frac{dC}{dt}$ represents the change in CO_2 concentration with time in a chemostat having a flow rate (F) in L h^{-1} and volume V in L. C_o , and C represents initial and instantaneous CO_2 concentration in g L^{-1} respectively, while C^* represents the concentration of CO_2 owing to its solubility at 25°C , in g L^{-1} . The terms X and $Y_{C/X}$ defines the instantaneous biomass concentration (g L^{-1}) and the mass of CO_2 consumed per mass of microalgae produced (g g^{-1}) respectively. $k_L a$ and μ signifies volumetric mass transfer coefficient of CO_2 in water in m day^{-1} and maximum specific growth rate in day^{-1} .

Eq. (5) illustrates the change in phosphorous concentration with time ($\frac{dP}{dt}$) in a reactor with flow rate (F) in L h^{-1} and volume (V) in L

$$\frac{dP}{dt} = \frac{F}{V} (P_o - P) - \mu X Y_{P/X} \quad (5)$$

Where P_o and P represents intial and instantaneous concentration of phosphorous in g L^{-1} , X and $Y_{P/X}$ defines the biomass concentration (g L^{-1}) and mass of phosphate consumed per algal biomass (g g^{-1}) respectively.

The exponential decline of light intensity inside the photobioreactor with the increase in depth is measured by Beer Lambert's Law as provided in Eq. (6) given below.

$$I = I_0 e^{-\zeta z} \quad (6)$$

Where, the terms I and I_0 corresponds to the light irradiance inside the BCPBR (W m^{-2}) with the variation in depth (z) in m, and solar irradiance received on the surface (W m^{-2}) respectively.

The solar irradiance received (I) on the surface of PBR was measured with an in-house ambient weather monitoring system. The absorption and transmission of the BCPBR's plexi-glass material was neglected since it was considered as totally transparent. The exponential decline of light intensity inside the photobioreactor (I_0) with the increase in depth (z) was calculated using Beer Lambert's law as mentioned above.

The term ζ represents the rate of light attenuation and is dependent over the biomass concentration, and can be expressed as Eq. (7) as follows

$$\zeta = aX + b \quad (7)$$

where X is the biomass concentration (g L^{-1}), a is specific light attenuation constant in $\text{m}^2 \text{g}^{-1}$ and b is the background turbidity (m^{-1}).

Chang et al., [37] have reported that 1% of urinary effluent contributes to 50 % load of phosphorus in domestic wastewater which contributes to eutrophication in freshwater ecosystems. Phosphorus influences the formation of Adenosine triphosphate (ATP), and several structural and biochemical components and thereby the cellular energetics and inherent algal growth. Also, the uptake and metabolism of phosphorus is dependent over other environmental factors like the light intensity and the temperature. In several freshwater ecosystems, the concentration of phosphorous, determines the growth of microalgae and development of algal blooms [38]. Thus, the present study utilized a simplified Monod model employing phosphate as the limiting nutrient along with the influencing light and temperature effects to predict the growth of microalgae using urinary effluent. The Monod model for growth kinetics was combined with the multiphase eulerian-eulerian CFD model to predict the hydrodynamics and algal growth in the bubble column photobioreactor. The idea is to biologically recover phosphorous efficiently via cultivation in BCPBR in the form of algal biomass, which could be applied as biofertilizer to address the issues of depleted phosphorous reserves.

2.4.3. Integration of kinetics in CFD simulations

A user-defined function based on the growth kinetic model for a BCPBR was written in C language and was integrated inside the Ansys Fluent v15 software [35]. The user-defined function initialized 4 scalar variables i.e. the initial biomass, CO_2 , limiting nutrient (i.e.) phosphate concentration, and light irradiance. This function runs simultaneously with CFD simulations of BCPBR. 1-time step was considered as 1 h inside the model during simulations. Photoperiod (Light: Dark [L:D]) of 14:10 was assumed and only the day time i.e 14 h (diurnal variation) were considered in the model to simulate biomass growth and nutrient uptake, since, the biomass growth is usually limited in the absence of light due to night time respiratory losses [39]. The death coefficient was also incorporated in the algal growth kinetic model to account for the decline in growth during the night. Therefore, the simulations were run for 84-time steps, i.e. a total of 6 days having 14 h day time each day, with 20 iterations each. The real-time solar irradiance data (14 h day time of each day) were fed in the model (Fig. S1). The variation in ambient air temperature during the period of growth was also monitored (Fig. S2), and the water temperature was measured by thermometer and fed into the kinetic model. The optimum water temperature has been assumed as 23°C , based on the study by Behera et al., [40]. The initial concentrations during the cultivation using 5.5 % (v/v) DHU have been set as initial user-defined scalar (UDS) values, with biomass (X_0), phosphate (P_0) and carbon dioxide (CO_2) [C_0] concentration of 0.079 g L^{-1} , 0.014 g L^{-1} and 0.0611 g L^{-1} respectively based on the experimental results. The initial irradiance value (I_0) has been set as 0 W m^{-2} .

The CFD simulations were run numerous times with different combination of calibration constants to find the best fitting predicted values to the experimental values. The combination of two curvefitting calibration constants; 6.75 multiplied to the equation estimating specific growth rate of microalgae and the second constant 0.8 multiplied to phosphate removal equation produced the least sum of squared errors and provided the best regression coefficient

Real-time solar from in-house ambient weather monitoring system was fed into the CFD model using text file. The mass transfer coefficient of CO_2 from the gas phase to the liquid phase was estimated from the protocol as reported by Akita and Yoshida [41]. The mass transfer coefficient 0.001832 s^{-1} is comparable to the one obtained by Pegal-lapati and Nirmalakhandan, [12], which are 0.0019 s^{-1} and 0.0024 s^{-1} for the flow rate of 800 mL min^{-1} and 1200 mL min^{-1} respectively. Since 5.5 % (v/v) DHU exhibited maximum growth, its data was used as the Monod's model constants inside the kinetic growth model. The

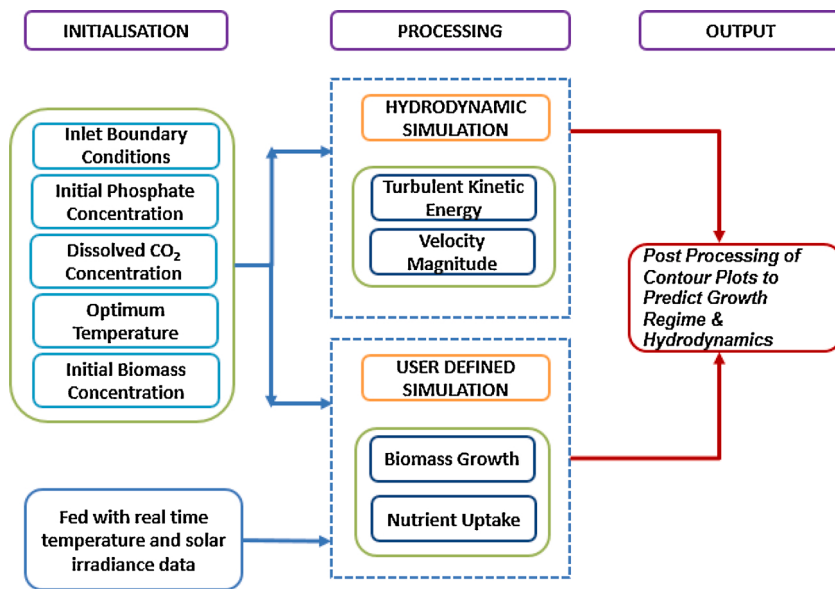


Fig. 1. Flowchart of the methodology adapted for predicting growth regime and hydrodynamics in BCPBR using CFD simulations.

Table 1
List of constants used in the kinetic model.

Parameters	Values	Reference
μ_{max} (Maximum specific growth rate)	0.814 d ⁻¹	This study
μ (Specific growth rate)	0.478 d ⁻¹	This study
D (Specific death rate)	0.004 d ⁻¹	Eze et al. [13]
K_s (Half saturation constant of phosphate)	10.53 mg L ⁻¹	Aslan and Kapdan [42],
K_c (Half saturation constant of CO ₂)	124.900 mg L ⁻¹	Zhang et al., [43]
K_l (Half saturation constant of irradiance)	26.0889 W m ⁻²	Diehl et al., [44]
K_{la} (Mass transfer coefficient of CO ₂)	0.001832 s ⁻¹	This study
D_b (Bubble diameter)	0.3 cm	Kommareddy et al., [45]
P_b (Pressure inside the bubble)	1.0566 atm	This study
K_h (Henry's law constant for CO ₂)	29.4 bar mol ⁻¹	Levy et al., [46]
D_L (Diffusivity)	0.0016 mm ² s ⁻¹	Versteeg and Swaaij, [47]
$Y_{P/X}$ (Yield coefficient of PO ₄)	0.013 g g of algae	This study
$Y_{C/X}$ (Yield coefficient of CO ₂)	1.821 g g of algae	Eze et al., [13]
a (Specific light attenuation constant)	0.050 m ² g ⁻¹	Jupsin et al., [48]
b (Background turbidity constant)	0.320 m ⁻¹	Jupsin et al., [48]
T_{opt} (Optimum water temperature for algal growth)	23 °C	This study
m (Emperical constant for non-optimal temperature)	0.004 K ⁻² (T < T _{opt}) 0.006 K ⁻² (T > T _{opt})	Park, [35]

overall flowchart of the process has been illustrated in Fig. 1. The constants and parameters incorporated inside the model have been listed in Table 1.

The computational memory required for one CFD simulation was between 170–180 megabytes. The use of Eulerian multiphase model instead of the Langrangian particle tracking model led to a reduction of computational load during the simulation. The drag and non-drag forces models, although being computationally expensive, were added in the multiphase simulations to resemble the actual hydrodynamic mixing. Moreover, the simulation of algal growth with the use of UDFs, which ran parallel to the hydrodynamic simulations also kept the computational load in check. A grid sensitivity test and time step size dependency test was also carried out to obtain accurate results at expense of lesser computational memory.

3. Results and discussion

3.1. Microalgal productivity in BCPBR

Algal biomass productivity in different concentrations of fresh DHU with only atmospheric air and 4% CO₂ enriched air sparging was analyzed for 6 days in a lab-scale BCPBR. Fresh real human urine was diluted to 4.5 % v/v, 5.5 % v/v, 6.5 % v/v and 8.5 % v/v and was fed into the reactor with atmospheric air. Among the various combinations attempted in the study, 5.5 % (v/v) DHU with 4% CO₂ enriched air and 6.5 % (v/v) DHU without CO₂ enriched air exhibited maximum microalgal growth.

The absence of an inorganic carbon source often results in a decline of phototrophic algal growth. The maximum biomass concentration of 0.41 g L⁻¹ was obtained in 6.5 % (v/v) of DHU. The cultivation in 4.5 % (v/v) and 8.5 % (v/v) DHU exhibited final biomass concentration of 0.39 g L⁻¹ and 0.34 g L⁻¹ respectively. The pH during the study stayed in the range of 8–10 for 6 days due to the low concentration of inorganic carbon, which reduced the pH by the formation of bicarbonate ions [49]. Moreover, the accumulation of dissolved oxygen inside the PBR also must have caused some inhibitory effects on cell growth.

The 5.5 % (v/v) DHU fed with 4% CO₂ enriched air, exhibited maximum final biomass concentration of 1.06 g L⁻¹, while an algal concentration of 1.04 g L⁻¹, 0.78 g L⁻¹, and 0.59 g L⁻¹ were observed in 4.5 % (v/v), 6.5 % (v/v) and 8.5 % (v/v) DHU respectively. Maximum biomass productivity of 0.14 g L⁻¹ day⁻¹ was obtained in 5.5 % v/v DHU. The rise in algal biomass concentration with time has been shown in Fig. 2a. The results depicted that CO₂ in gaseous form is the feasible source of inorganic carbon for algal growth and is a very crucial factor that affects its growth. The forms of CO₂ (i.e. CO₂, H₂CO₃, HCO₃⁻, CO₃²⁻) in the liquid culture depend on the pH of the media [49]. In this case, HCO₃⁻ must have dominated inside the culture since the partial pressure of CO₂ in every bubble was mathematically estimated to be 4.10*10⁻² atm and the pH ranged between 6–7.

Keeping the environmental conditions like the light intensity and temperature constant, usually the concentration and uptake of inorganic nutrients plays an essential role in determining algal growth. The maximum ammonium concentration after the hydrolysis of urea reached about 0.92 mg/mL during the growth of microalgae in 5.5 % DHU which is lesser than the maximum ammonium concentration of 0.97 mg/mL and 1.03 mg/mL achieved during the growth in 6.5 % and 8.5 %. High concentration of ammonium nitrogen are toxic and inhibit the

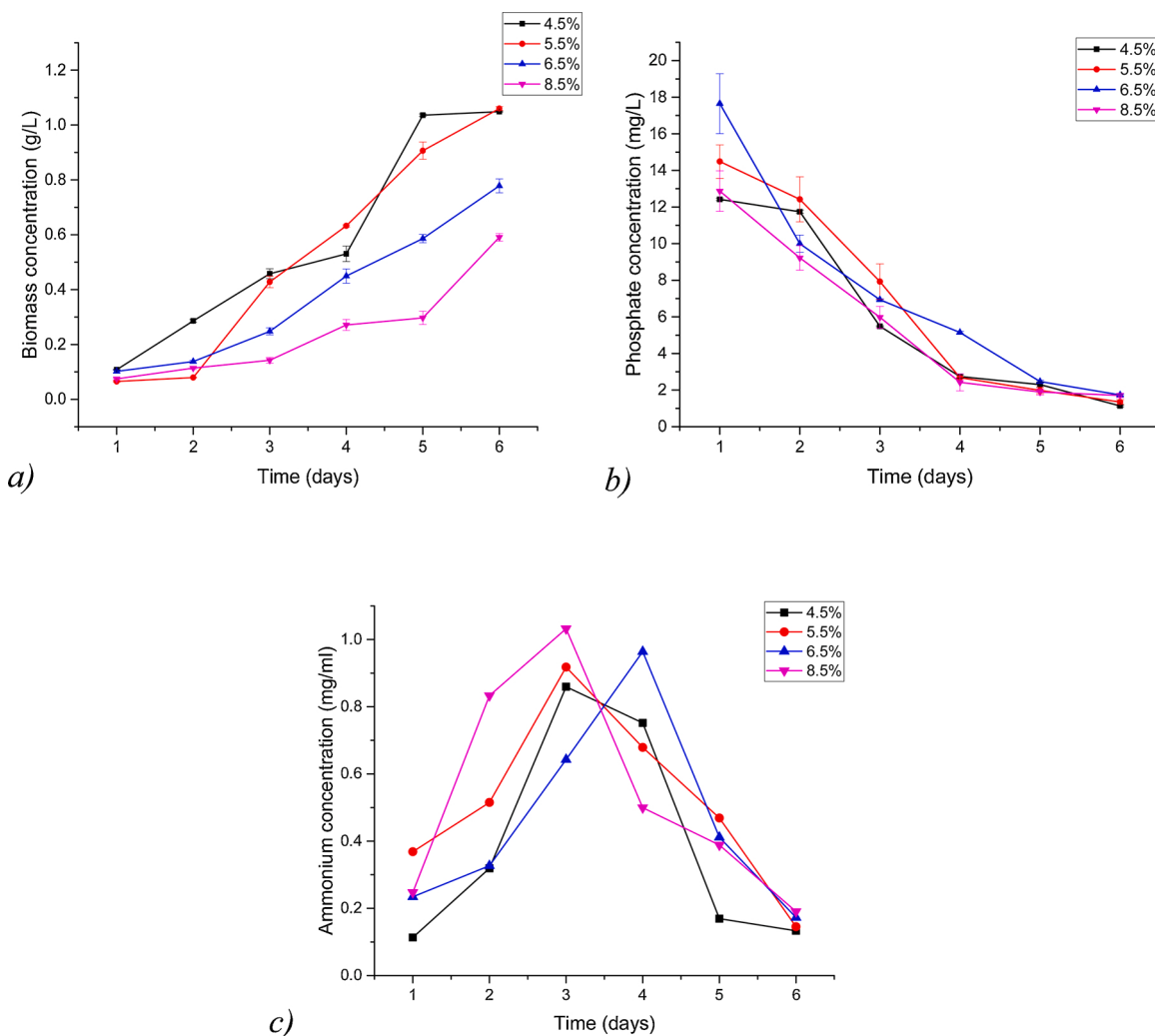


Fig. 2. Performance evaluation of BCPBR supplemented with 4% CO₂ enriched air for a). Microalgal content b). Phosphate depletion and c). Ammonium depletion under various concentrations of DHU.

microalgae growth [3,37], while a low concentration often declines the overall growth rate. An optimum level of ammonium ions is essential for metabolic conversion and assimilation into algal biomass. The phosphate removal is also influenced by the presence of free ammonium ions, where an optimum concentration of these ions also facilitates the uptake of phosphate ions that comprises the structural and biochemical content and thereby the overall algal growth rate [50]. 5.5 % v/v DHU had pH in the requisite range of 6–7 thus, providing nutrients in appropriate ionic form for efficient diffusion and assimilation by algal cells [6]. Thus, the maximal growth was observed in case of 5.5 % (v/v) DHU compared to the other dilutions.

Growth of *Chlorella vulgaris* with a final biomass concentration of 0.57 g L⁻¹ has been reported over 21 days, with no air sparging, in 1:25 dilution of human urine [3]. High biomass concentration of 16 g L⁻¹ of *Chlorella sorokiniana* has been reported by Tuanter et al., [4] in PBR with short optical paths with a working volume of 0.9 L in a controlled environment. Marbelia et al., [51] have compared the growth of *Chlorella vulgaris* in bubble column PBR and membrane PBR, with a working volume of 25 L and projected maximum algal productivity of 0.033 ± 0.009 g L⁻¹ day⁻¹ in bubble column PBR, which was slightly lower than that reported with membrane PBR.

Compared to the previously reported studies, high biomass productivity of 0.14 g L⁻¹ day⁻¹ and final algal concentration of 1.06 g L⁻¹ was achieved in a short period of 6 days with bubble column PBR under ambient conditions in the present study. The high biomass productivity

obtained might be attributed to the fact that microalgal species are well acclimatized with the nutrients present in urine and to the local environmental conditions. This represents an economical way of producing a high concentration of algal biomass as fresh diluted human urine was used in the medium and there were no additional expenses involved in controlling the environment in which the microalgae were cultivated. A more intensive study can help in scaling up of PBR designs to sequester CO₂ and produce high algal biomass concentration simultaneously in outdoor conditions more efficiently for obtaining a multitude of products in a biorefinery model.

3.2. Nutrient uptake efficiency of microalgae in BCPBR

The growth of microalgae is often supplemented by the simultaneous removal of nutrients, mainly nitrogen and phosphorous. The phosphate and ammonium removal by the microalgae in bubble column PBR was studied for 6 days as represented in Fig. 2b and c. Since ammonium ions are the main source of nitrogen in urine, only the uptake of ammonium-nitrogen was estimated. As the growth in PBR without CO₂ enrichment was found to be less, the results of ammonium and phosphate removal were reported to be very inconsistent. The pH value was also found to rise rapidly to 10, due to the absence of an inorganic carbon source. The high pH range (8–10) might have led to struvite precipitation and ammonia volatilization, thus declining the overall algal growth rate [13]. As evident from Fig. 2b about 90.9 %, 90.7 % 90.1 % and 86.7 % of

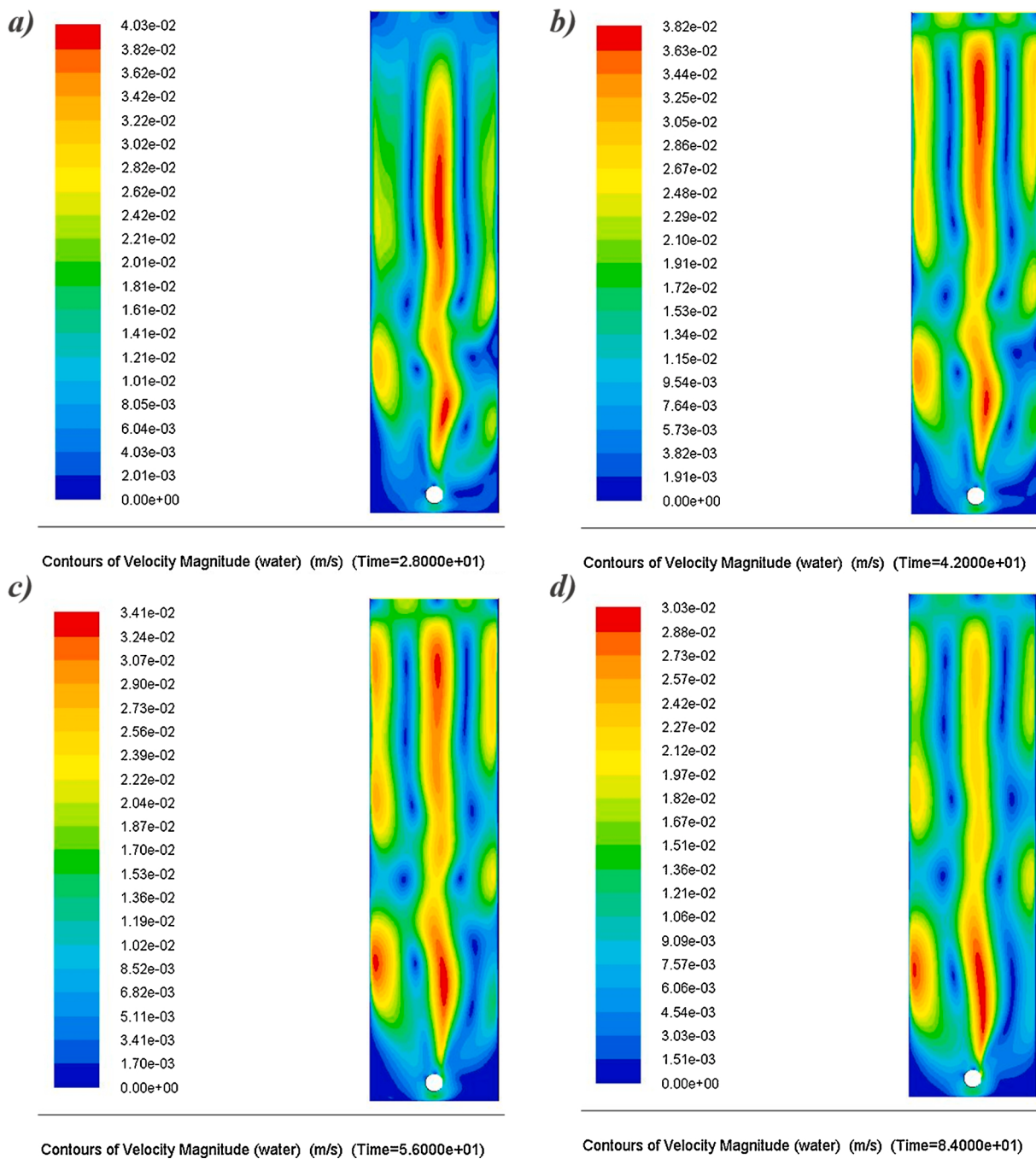


Fig. 3. Contours of water velocity magnitude in BCPBR at a) 28 h and b) 42 h; c) 56 h; d) 84 h.

phosphate was removed from 4.5 %, 5.5 %, 6.5 % and 8.5 % (v/v) of DHU respectively over 6 days when 4% v/v CO₂ enriched air was fed into the reactor.

Urea converts into ammonium and bicarbonate due to hydrolysis of urine, thus leading to an increase in ammonium ions as evident from Fig. 2c until 3rd day. As the algal growth increases over time, there is a gradual decline in ammonium concentration, as it is being used and metabolized by microalgae. About 84.60 %, 84.10 %, 82.10 % and 84.20 % removal of ammonium was achieved from 4.5 %, 5.5 %, 6.5 % and 8.5 % (v/v) of DHU respectively after the 6 days of study period. Similar trends of observations in the concentration of total nitrogen have been reported by Jaatinen et al., [3] for *Chlorella vulgaris* in DHU. The removal can be attributed to both microalgae consumption of nitrogen in the form of ammonia and ammonia volatilization out of the reactor.

Tuantet et al., [4] reported a 100 % phosphate and 71 % ammonium-nitrogen removal efficiency at a dilution rate of 0.05 h⁻¹ in a short light path PBR by *Chlorella sorokiniana* cultivated under controlled environment. Chang et al., [37] have reported removal efficiency of 96.50 % of total phosphorus and 97 % of ammonium nitrogen, within 7 days by *Spirulina platensis* cultivated in 120 times DHU media. Since the algal consortium was well acclimatized in urine, high biomass productivity with 90.80 % phosphate and 84.60 % ammonium-nitrogen removal from the media in a short period of 6 days was achieved. Thus, the results depict the high potential of BCPBR for low-cost phosphate and ammonium-nitrogen removal from source-separated urine with continuous operation, thereby reducing the load of conventional wastewater treatment plants. Though the operation of BCPBR due to the associated energy penalty because of the

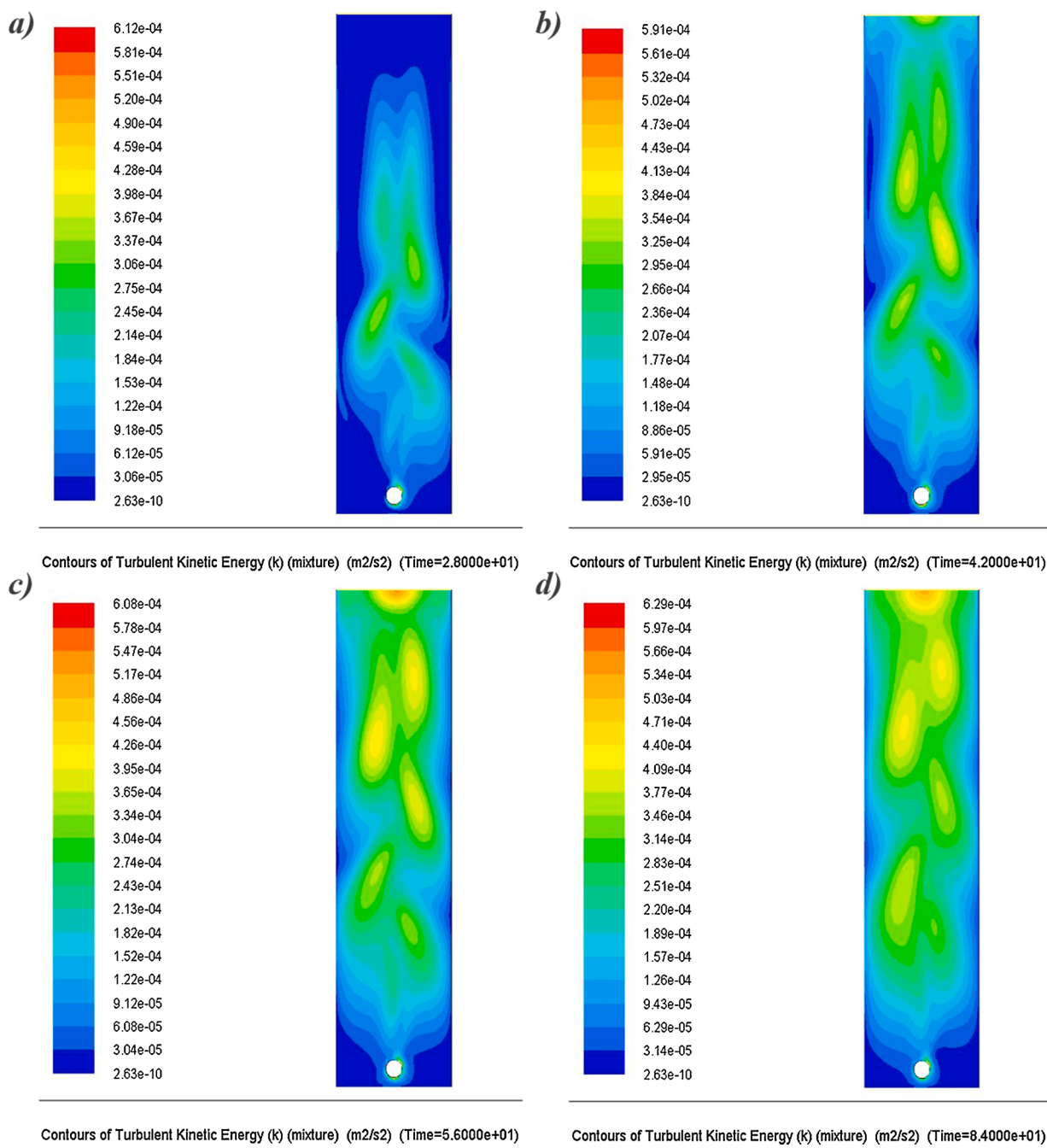


Fig. 4. Contours of turbulent kinetic energy in BCPBR at a) 28 h and b) 42 h; c) 56 h; d) 84 h.

back-pressure drop is regarded as costly, the utilization of waste resource for nutrient recovery and assimilation into algal biomass that can be processed to a multitude of products can be utilized for improvising the process economics.

3.3. Carbon dioxide biofixation by microalgae in BCPBR

The enzyme carbonic anhydrase is responsible for catalyzing the hydration of CO₂ into HCO₃⁻ and a proton, out of which the HCO₃⁻ is taken up by the microalgae to fulfill its carbon requirement [31]. The algal biomass was found to have 47.41 % carbon content. The reported carbon percentage of *Chlorella vulgaris* is usually in the range of 45 %-51 % [52]. Since the consortium was mostly dominated by *Chlorella sp.*, the data obtained can be correlated with that of the available literature.

The biofixation achieved in six days, during the cultivation in 5.5 %

DHU, by supplying 4% of CO₂ enriched air was 0.29 g L⁻¹ day⁻¹, resulting in maximum biomass concentration of 1.06 g L⁻¹. Razzak et al., [30] reported a maximum CO₂ biofixation of 0.197 g L⁻¹ d⁻¹ through the cultivation of *Chlorella vulgaris* in a vertical tubular PBR after 5 days by supplying 4% CO₂ enriched air. The lesser carbon content (i.e.) 40.7 % of *C. vulgaris* must have resulted in a lower biofixation efficiency than the current study. Adamczyk et al., [52] reported maximum biomass productivity of 0.71 g L⁻¹ day⁻¹ with CO₂ fixation of 0.25 g L⁻¹ day⁻¹ by cultivating *Chlorella vulgaris* in a 15 L tubular reactor, within 10 days with the supply of 4% CO₂ enriched air. Sydney et al., [31] reported a CO₂ fixation rate of *C. vulgaris* of 0.25 g L⁻¹ day⁻¹ in 12 days with a 5% supply of CO₂ enriched air, using a biofermentor having 8 L working volume.

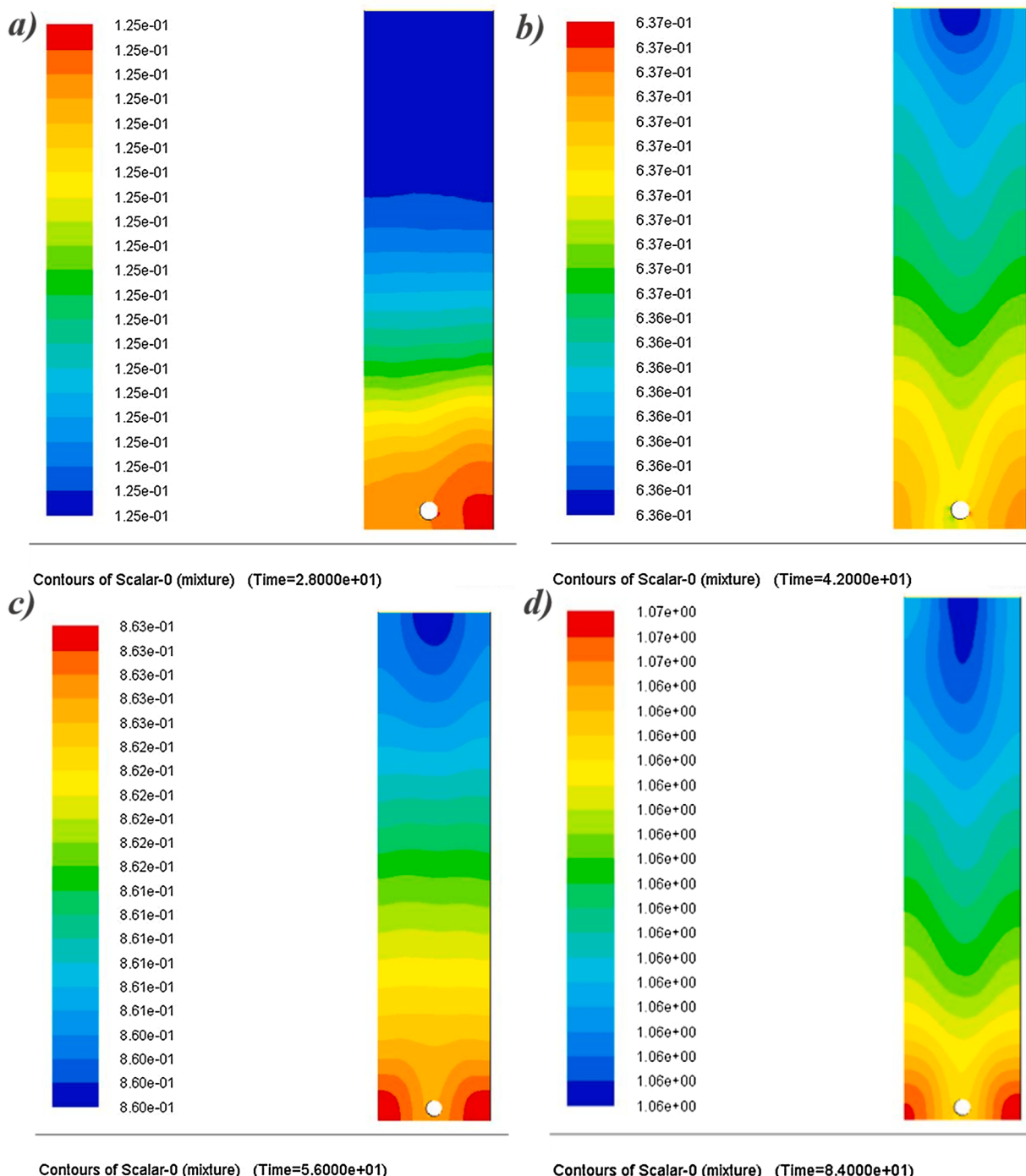


Fig. 5. Contour of predicted biomass in BCPBR after a) 28 h (0.357 g L^{-1}); b) 42 h (0.637 g L^{-1}); c) 56 h (0.863 g L^{-1}); d) 84 h (1.06 g L^{-1}).

3.4. CFD simulations

Hydrodynamics and biomass growth inside the reactor were simulated with the help of CFD. The post-processing of data was used to analyze the contours of hydrodynamic characteristics inside the BCPBR.

3.4.1. Water velocity contours

Water velocity depends on the gas hold up and flow rate of the aeration. The simulation result of the shape and movement of the bubble plume often resembles the actual hydrodynamics inside the reactor. The contours of water velocity for 28 h, 42 h, 56 h, and 84 h are represented in Fig. 3a-d respectively. Over time, with the increase in algal cell

density, the maximum velocity magnitude was found to decrease. The simulations also showed mixing similar to the actual conditions inside the BCPBR. The movement of water tracked with the help of vectors displayed efficient circular mixing inside the reactor. The water was found to rise along with the bubble plume and then descends from all sides. This could also be verified by the maximum air velocity of 4.03 cm s^{-1} , 3.82 cm s^{-1} , 3.41 cm s^{-1} and 3.03 cm s^{-1} obtained just above the sparger (red region) at 28 h, 42 h, 56 h, and 84 h respectively. The down-comer velocity at 28 h, 42 h, 56 h and 84 h was recorded as 2.01 cm s^{-1} , 1.91 cm s^{-1} , 1.36 cm s^{-1} , and 1.51 cm s^{-1} respectively. Higher shear stress zones were found to be located close to the region of the gas inlet and the riser. The formation of a few eddies near the walls of the reactor

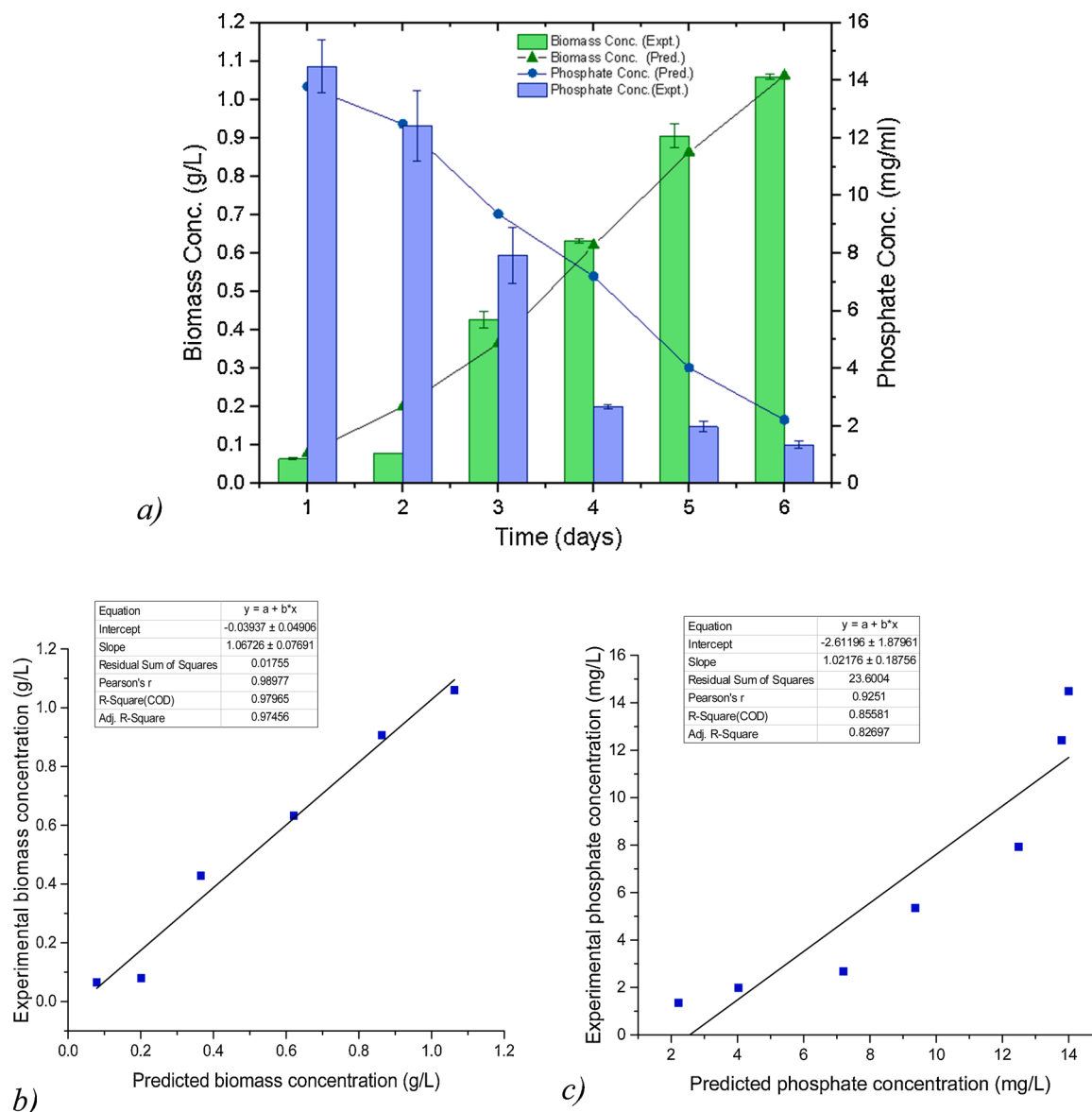


Fig. 6. a). Comparision of experimental vs predicted values for biomass content and phosphate removal with time; Curve fitting of experimental and predicted values of b). biomass content c). phosphate removal in BCPBR.

also depicts efficient mixing. The air gets degassed out of the 2-D geometry as the degassing condition is applied. Syed et al., [53] reported a homogenous regime in an air-water bubble column reactor with a superficial velocity of 0.038 m s^{-1} using CFD simulations. Gao et al., [22] have reported the velocity contours inside the airlift PBR and have taken into consideration the gas hold-up, virtual mass, and turbulent dispersion forces, thus projecting their influence in modulating the shear stress and thereby the algal growth.

3.4.2. Turbulent kinetic energy contours

Turbulent kinetic energy is the index that notifies the development or decline of turbulence [54]. Turbulence provides efficient mixing inside the reactor, which helps in mass and heat transfer between the phases. However, excess turbulence can produce enough shear forces that may damage the cell wall of microalgae [8]. The maximum turbulent kinetic energy at 28th, 42nd, 56th and 84th time step was reported as $0.000612 \text{ m}^2 \text{ s}^{-2}$, $0.000591 \text{ m}^2 \text{ s}^{-2}$, $0.000608 \text{ m}^2 \text{ s}^{-2}$, and $0.000629 \text{ m}^2 \text{ s}^{-2}$ respectively. Maximum turbulence was observed at the top of the reactor owing to the phenomenon of bubble breakage at the air-water interface. The healthy and exponential growth of microalgae

indicated that the turbulence was not high enough to damage the cell walls since, the flow rate was maintained at 0.14 vvm as mentioned before to avoid the effects of shear stress on microalgae growth [32]. The green microalgae are least sensitive to inhibition in the growth by turbulence [55]. The contours of the turbulent kinetic energy (Fig. 4a-d) depicts thorough mixing all over the reactor except in the bottom which can be correlated to the settling of microalgae at the base of the reactor. Li and Li, [56] used CFD simulations to predict the turbulence inside the BCPBR and projected it to be a complex function of the sparger nozzle along with the liquid and gas viscosity inside the BCPBR. Gao et al., [22] reported the essentiality of maintaining adequate gas velocity and turbulence inside the reactor for avoiding inhibition of algal growth inside an airlift PBR.

3.4.3. Validation of microalgal growth and nutrient uptake prediction

Fig. 5 (a-d) of contours inside the BCPBR exhibit the biomass growth as predicted by the model, which has been integrated with the hydrodynamics of the reactor. The biomass concentration as predicted by the model after 2nd day (28 h) was 0.36 g L^{-1} , and subsequently found to be 0.63 g L^{-1} after 3rd day (42 h), 0.86 g L^{-1} after 4th day (56 h) and 1.07 g L^{-1} after 6th day (72 h). The phosphate removal was found to be 14.5 mg ml^{-1} after 1st day (28 h), 9.5 mg ml^{-1} after 2nd day (42 h), 7.0 mg ml^{-1} after 3rd day (56 h), 5.5 mg ml^{-1} after 4th day (72 h), 4.0 mg ml^{-1} after 5th day (88 h) and 2.5 mg ml^{-1} after 6th day (104 h).

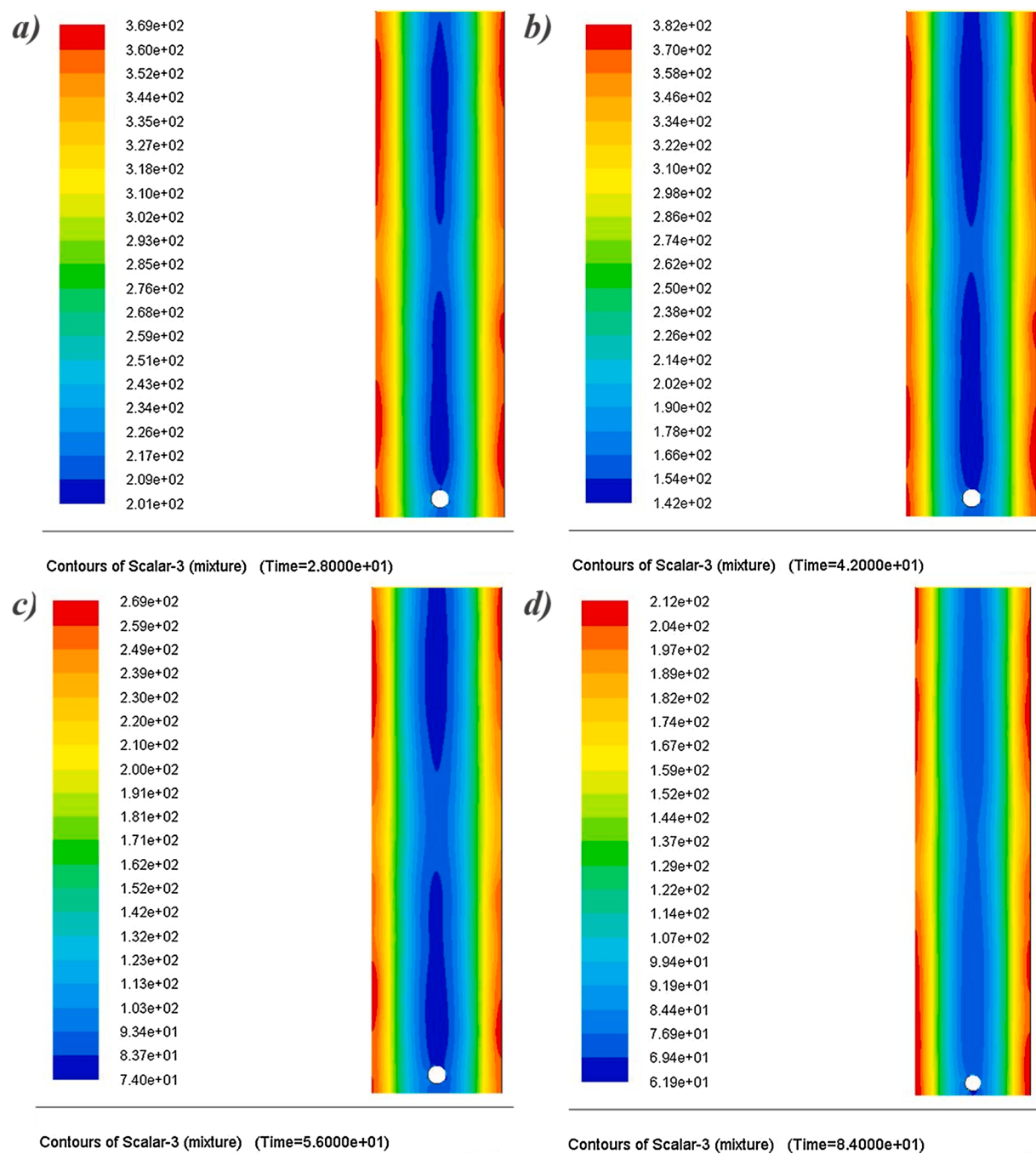


Fig. 7. Contours of light irradiance in BCPBR at a) 28 h; b) 42 h; c) 56 h; and d) 84 h.

L^{-1} at the end of 6th day (84 h). The predicted phosphate concentration after removal on 2nd day was 0.012 g L^{-1} , 0.010 g L^{-1} on the 3rd day, while on 4th and 6th day it was 0.00729 g L^{-1} and 0.002 g L^{-1} respectively. The validation of the data obtained from simulations with the experimental study of biomass growth and nutrient removal inside the PBR with 5.5 % (v/v) DHU enriched with 4% (v/v) of CO_2 enriched air showed that the kinetic model developed was accurate in predicting the variations in biomass concentration and phosphate removal (Fig. 6a). The graphs corresponding to the correlation between the experimental and predicted values from CFD for changes in algal biomass and phosphate concentration in the media over time are represented in Fig. 6b and c respectively. R^2 of 0.98 depicted that the model accurately predicted the changes in algal concentration with time and the inclusion of hydrodynamics helped in providing more efficient real-

time predictions. The addition of the effects of varying real-time solar irradiance and temperature into the model made it follow the trend of biomass growth coherently. Similar to the present study, Gao et al., [22] reported that the photosynthetic growth rate of algae increases during the initial period and then shifts from the low illuminated center towards the illuminated boundary region. The low R^2 value of 0.82 obtained for phosphate removal might be attributed to the precipitation of struvite during the growth period of algae. Eze et al., [13] have reported 98 % and 97 % accuracy of biomass and nutrient removal prediction respectively compared to the present model by incorporating parameters like pH prediction, effects of ammonia volatilization, and its oxidation to nitrate. Pegallapati and Nirmalakhandan, [12] have reported R^2 value of 0.87 ensuring goodness of fit between the model and experimental values with *Scenedesmus sp.* in internally illuminated PBR

with an 800 mL min⁻¹ flow rate of 4% (v/v) CO₂ enriched air.

3.4.4. Light distribution inside BCPBR

Fig. 7 (a-d) represented the light distribution inside the reactor, starting from the 2nd day (28 h) until the 6th day (84 h). Light distribution was found to be maximum at the walls i.e. 369 W m⁻² (763 μmol m⁻²s⁻¹), 382 W m⁻² (790 μmol m⁻²s⁻¹), 269 W m⁻² (556 μmol m⁻²s⁻¹), and 212 W m⁻² (438 μmol m⁻²s⁻¹) at the end of 2nd day (28 h), 3rd day (42 h), 4th day (56 h) and 6th day (84 h) respectively. As evident from the contours, the center portion of the reactor showed the minimum light irradiance values of 201 W m⁻² (416 μmol m⁻²s⁻¹), 142 W m⁻² (293 μmol m⁻²s⁻¹), 74 W m⁻² (153 μmol m⁻²s⁻¹), and 61 W m⁻² (126 μmol m⁻²s⁻¹) at the end of 28 h, 42 h, 56 h, and 84 h respectively. An increase in algal culture density over time resulted in gradual light attenuation from the periphery of the reactors towards the center. A similar trend has been reported by **Komareddy and Ananthula**, [57] using the discrete ordinates (DO) irradiance model in an airlift PBR. Microalgal cells at the center of the PBR receive relatively lower irradiance compared to the cells at the wall of PBR due to light attenuation, and a better mixing can provide adequate exposure of light to all the cells. **Nuaha and Alopaeus**, (2013) also reported that even though the light intensity is more on the walls, compared to other regions of the BCPBR, an adequate mixing can result in uniform growth of algal cells throughout the reactor. Therefore, by examining the contours of biomass growth, mixing (velocity and turbulent kinetic energy), and light distribution, improvements can be made in the design of PBRs of various geometries during scale-up [58] for achieving better algal productivity. The nexus of such simple and efficient models with CFD simulations can make the process of designing PBRs at large-scale far easier and quicker.

4. Conclusion

Native microalgal consortium dominated by *Chlorella sp.* was cultivated in BCPBR using DHU. Maximum algal productivity of 0.14 g L⁻¹ day⁻¹ with a growth rate of 0.48 day⁻¹ resulting in the removal of 90.70 % and 84.10 % of phosphate and ammonium using 5.5 % (v/v) DHU with 4% CO₂ enriched air. CFD simulations via integrating the kinetics of algal growth with the BCPBR hydrodynamics predicted the algal concentration and phosphate removal with an accuracy of 98 % and 82 % respectively. Contours of hydrodynamics, algal growth, and light irradiance of the BCPBR would provide relevant information to facilitate the easier designing of PBRs for commercial-scale application of microalgae.

Authors' contribution

PB has initiated the concept of the project. SSP and BB have done the experiments and collected the data for interpretation. SSP has developed the CFD codes and performed the simulations. SJ has interpreted the CFD simulations. SSP and BB have drafted the manuscript. PB and SJ has reviewed and finalized the manuscript. All authors read and approved the final manuscript for peer review and possible publication.

Declaration of Competing Interest

The authors report no declarations of interest.

Acknowledgments

The authors thank the Department of Biotechnology and Medical Engineering and the Department of Chemical Engineering of National Institute of Technology (NIT) Rourkela for providing the necessary research facilities. The authors thank the Ministry of Human Resources and Development (MHRD) of the Government of India (GoI) for providing the fellowship to the first and the second author for Master's and Doctoral degrees respectively. The authors greatly acknowledge the

Department of Science and Technology under ASEAN-India Science, Technology & Innovation Cooperation [File No. IMRC/AISTDF/CRD/2018/000082] for sponsoring the research grant.

Appendix A. Supplementary data

Supplementary material related to this article can be found, in the online version, at doi:<https://doi.org/10.1016/j.jece.2020.104615>.

References

- [1] N. Azhand, A. Sadeghzadeh, R. Rahimi, Effect of superficial gas velocity on CO₂ capture from air by *Chlorella vulgaris* microalgae in an Airlift photobioreactor with external sparger, *J. Env. Chem. Eng.* 8 (2020), 104022.
- [2] B. Behera, N. Aly, P. Balasubramanian, Biophysical model and techno-economic assessment of carbon sequestration by microalgal ponds in Indian coal based power plants, *J. Clean. Prod.* 221 (2019) 587–597.
- [3] S. Jaatinen, A.M. Lakaniami, J. Rintala, Use of diluted urine for cultivation of *Chlorella vulgaris*, *Environ. Technol.* 37 (2016) 1159–1170.
- [4] K. Tuantet, H. Temmink, G. Zeeman, R.H. Wijffels, C.J. Buisman, M. Janssen, Optimization of algae production on urine, *Algal Res.* 44 (2019) 1–11.
- [5] K. Tuantet, H. Temmink, G. Zeeman, M. Janssen, R.H. Wijffels, C.J. Buisman, Nutrient removal and microalgal biomass production on urine in a short light-path photobioreactor, *Water Res.* 55 (2014) 162–174.
- [6] B. Behera, S. Patra, P. Balasubramanian, Biological nutrient recovery from human urine by enriching mixed microalgal consortium for biodiesel production, *J. Environ. Manage.* 260 (2020) 1–31.
- [7] B. Behera, A. Acharya, I.A. Gargay, N. Aly, P. Balasubramanian, Bioprocess engineering principles of microalgal cultivation for sustainable biofuel production, *Bioresour Technol Rep.* 5 (2019) 297–316.
- [8] L. López-Rosales, F. García-Camacho, A. Sánchez-Mirón, A. Contreras-Gómez, E. Molina-Grima, Modeling shear-sensitive dinoflagellate microalgae growth in bubble column photobioreactors, *Bioresour. Technol.* 245 (2017) 250–257.
- [9] C.E. de Farias Silva, R.B. de Oliveira Cerqueira, C.F. de Lima Neto, F.P. de Andrade, F. de Oliveira Carvalho, J. Tonholo, Developing a kinetic model to describe wastewater treatment by microalgae based on simultaneous carbon, nitrogen and phosphorous removal, *J. Environ. Chem. Eng.* 8 (2020), 103792.
- [10] H.T. Hsueh, W.J. Li, H.H. Chen, H. Chu, Carbon bio-fixation by photosynthesis of *Thermosynechococcus* sp. CL-1 and *Nannochloropsis* occulata, *J. Photochem. Photobiol. B* 95 (2009) 33–39.
- [11] L. Xin, H. Hong-Ying, G. Ke, S. Ying-Xue, Effects of different nitrogen and phosphorus concentrations on the growth, nutrient uptake, and lipid accumulation of a freshwater microalga *Scenedesmus* sp., *Bioresour. Technol.* 101 (2010) 5494–5500.
- [12] A.K. Pegallapati, N. Nirmalakhandan, Modeling algal growth in bubble columns under sparging with CO₂-enriched air, *Bioresour. Technol.* 124 (2012) 137–145.
- [13] V.C. Eze, S.B. Velasquez-Orta, A. Hernández-García, I. Monje-Ramírez, M.T. Ortíz-Ledesma, Kinetic modelling of microalgae cultivation for wastewater treatment and carbon dioxide sequestration, *Algal Res.* 32 (2018) 131–141.
- [14] E. Lee, M. Jalalizadeh, Q. Zhang, Growth kinetic models for microalgae cultivation: a review, *Algal Res.* 12 (2015) 497–512.
- [15] P. Darvehei, P.A. Bahri, N.R. Moheimani, Model development for the growth of microalgae: a review, *Renew Sustain Energ. Rev.* 97 (2018) 233–258.
- [16] X. Gao, B. Kong, R.D. Vigil, Simulation of algal photobioreactors: recent developments and challenges, *Biotechnol. Lett.* 40 (2018) 1311–1327.
- [17] Q. Huang, F. Jiang, L. Wang, C. Yang, Design of photobioreactors for mass cultivation of photosynthetic organisms, *Eng. J.* 3 (2017) 318–329.
- [18] E.K. Nauha, V. Alopaeus, Modeling method for combining fluid dynamics and algal growth in a bubble column photobioreactor, *Chem. Eng. J.* 229 (2013) 559–568.
- [19] E.K. Nauha, V. Alopaeus, Modeling outdoors algal cultivation with compartmental approach, *Chem. Eng. J.* 259 (2015) 945–960.
- [20] H. Hadiyanto, S. Elmore, T. Van Gerven, A. Stankiewicz, Hydrodynamic evaluations in high rate algae pond (HRAP) design, *Chem. Eng. J.* 217 (2013) 231–239.
- [21] R. Heisz, B. Sialve, B. Morchain, R. Escudé, J.P. Steyer, P. Guiraud, Experimental and numerical investigation of hydrodynamics in raceway reactors used for algaculture, *Chem. Eng. J.* 250 (2014) 230–239.
- [22] X. Gao, B. Kong, R.D. Vigil, Multiphysics simulation of algal growth in an airlift photobioreactor: effects of fluid mixing and shear stress, *Bioresour. Technol.* 251 (2018) 75–83.
- [23] X. Gao, B. Kong, R.D. Vigil, Comprehensive computational model for combining fluid hydrodynamics, light transport and biomass growth in a Taylor vortex algal photobioreactor: eulerian approach, *Algal Res.* 24 (2017) 1–8.
- [24] X. Gao, Advanced CFD Model of Multiphase Photobioreactors for Microalgal Derived Biomass Production, Iowa State University, Ames, Iowa, 2016, pp. 1–205.
- [25] M. Prussi, M. Buffi, D. Casini, D. Chiaramonti, F. Martelli, M. Carnevale, M. R. Tredici, L. Rodolfi, Experimental and numerical investigations of mixing in raceway ponds for algae cultivation, *Biomass Bioenergy* 67 (2014) 390–400.
- [26] G. Olivieri, L. Gargiulo, P. Lettieri, L. Mazzei, P. Salatino, A. Marzocchella, Photobioreactors for microalgal cultures: a Lagrangian model coupling hydrodynamics and kinetics, *Biotechnol. Prog.* 31 (2015) 1259–1272.
- [27] J. Huang, J. Ying, F. Fan, Q. Yang, J. Wang, Y. Li, Development of a novel multi-column airlift photobioreactor with easy scalability by means of computational

- fluid dynamics simulations and experiments, *Bioresour. Technol.* 222 (2016) 399–407.
- [28] B. Behera, K. Nageshwari, M. Darshini, P. Balasubramanian, Evaluating the harvesting efficiency of inorganic coagulants on native microalgal consortium enriched with human urine, *Water Sci. Technol.* (2020) 1–10.
- [29] G.L. Miller, Modified DNS method for reducing sugars, *Anal. Chem.* 31 (1959) 426–428.
- [30] S.A. Razzak, S.A.M. Ali, M.M. Hossain, A.N. Mouanda, Biological CO₂ fixation using Chlorella vulgaris and its thermal characteristics through thermogravimetric analysis, *Bioproc Biosyst Eng.* 39 (2016) 1651–1658.
- [31] E.B. Sydney, A.C.N. Sydney, J.C. de Carvalho, C.R. Soccol, Potential carbon fixation of industrially important microalgae. *Biofuels From Algae*, Elsevier, 2019, pp. 67–88.
- [32] C.G. Khoo, M.K. Lam, K.T. Lee, Pilot-scale semi-continuous cultivation of microalgae Chlorella vulgaris in bubble column photobioreactor (BC-PBR): hydrodynamics and gas–liquid mass transfer study, *Algal Res.* 15 (2016) 65–76.
- [33] G.M. da Rosa, L. Moraes, J.A.V. Costa, Spirulina cultivation with a CO₂ absorbent: influence on growth parameters and macromolecule production, *Bioresour. Technol.* 200 (2016) 528–534.
- [34] K. Ekambara, R.S. Sanders, K. Nandakumar, J.H. Masliyah, CFD modeling of gas–liquid bubbly flow in horizontal pipes: influence of bubble coalescence and breakup, *Int. J. Chem. Eng.* 2012 (2012) 1–21.
- [35] S.Y. Park, Modeling and Experimental Study of an Open Channel Raceway System to Improve the Performance of *Nannochloropsis* Salina Cultivation Doctoral Dissertation, The Ohio State University, 2014, pp. 1–176.
- [36] S.C. James, V. Boriah, Modeling algae growth in an open-channel raceway, *J. Comput. Biol.* 17 (2010) 895–906.
- [37] Y. Chang, Z. Wu, L. Bian, D. Feng, D.Y. Leung, Cultivation of *Spirulina platensis* for biomass production and nutrient removal from synthetic human urine, *Appl. Energ.* 102 (2013) 427–431.
- [38] W.S. Beck, E.K. Hall, Confounding factors in algal phosphorus limitation experiments, *PLoS One* 13 (10) (2018), e0205684.
- [39] A. Otondo, B. Kokabian, S. Stuart-Dahl, V.G. Gude, Energetic evaluation of wastewater treatment using microalgae, *Chlorella vulgaris*, *J. Environ. Chem. Eng.* 6 (2018) 3213–3222.
- [40] B. Behera, N. Aly, P. Balasubramanian, Biophysical modeling of microalgal cultivation in open ponds, *Ecol. Model.* 388 (2018) 61–71.
- [41] K. Akita, F. Yoshida, Gas holdup and volumetric mass transfer coefficient in bubble columns. Effects of liquid properties, *Ind. Eng. Chem. Process Des. Dev.* 12 (1973) 76–80.
- [42] S. Aslan, I.K. Kapdan, Batch kinetics of nitrogen and phosphorus removal from synthetic wastewater by algae, *Ecol. Chem. Eng. S* 28 (2006) 64–70.
- [43] Q.H. Zhang, X.C. Wang, J.Q. Xiong, R. Chen, B. Cao, Application of life cycle assessment for an evaluation of wastewater treatment and reuse project—Case study of Xi'an, China. *Bioresour. Technol.* 101 (2010) 1421–1425.
- [44] S. Diehl, S. Berger, R. Wöhrl, Flexible nutrient stoichiometry mediates environmental influences on phytoplankton and its resources, *Ecology*. 86 (2006) 2931–2945.
- [45] A.R. Kommareddy, G.A. Anderson, S.P. Gent, G.S. Bari, The impact of air flow rate on photobioreactor Sparger/Diffuser bubble size (s) and distribution. 2013 Kansas City, Missouri, July 21–July 24, American Society of Agricultural and Biological Engineers, 2013, p. 1.
- [46] J.B. Levy, F.M. Hornack, M.A. Levy, Simple determination of Henry's law constant for carbon dioxide, *J. Chem. Educ.* 64 (260) (1987) 1–2.
- [47] G.F. Versteeg, W.P. Van Swaaij, Solubility and diffusivity of acid gases (carbon dioxide, nitrous oxide) in aqueous alkanolamine solutions, *J. Chem. Eng.* 33 (1988) 29–34.
- [48] H. Jupsin, E. Praet, J.L. Vasel, Dynamic mathematical model of high rate algal ponds (HRAP), *Water Sci. Technol.* 48 (2003) 197–204.
- [49] J. Fu, Y. Huang, Q. Liao, A. Xia, Q. Fu, X. Zhu, Photo-bioreactor design for microalgae: a review from the aspect of CO₂ transfer and conversion, *Bioresour. Technol.* 292 (2019) 1–12.
- [50] A. Beuckels, E. Smolders, K. Muylaert, Nitrogen availability influences phosphorus removal in microalgae-based wastewater treatment, *Water Res.* 77 (2015) 98–106.
- [51] L. Marbelia, M.R. Bilad, I. Passaris, V. Discart, D. Vandamme, A. Beuckels, I. F. Vankelecom, Membrane photobioreactors for integrated microalgae cultivation and nutrient remediation of membrane bioreactors effluent, *Bioresour. Technol.* 163 (2014) 228–235.
- [52] M. Adamczyk, J. Lasek, A. Skawińska, CO₂ biofixation and growth kinetics of *Chlorella vulgaris* and *Nannochloropsis gaditana*, *Appl. Biochem. Biotechnol.* 179 (2016) 1248–1261.
- [53] A.H. Syed, M. Boulet, T. Melchiori, J.M. Lavoie, CFD simulations of an air–water bubble column: effect of Luo coalescence parameter and breakup kernels, *Front. Chemistry* 5 (2017) 68–84.
- [54] L. Li, J.Y. Zhu, J.F. Rong, W. Liu, C.G. Bai, Study on turbulent kinetic energy in closed photobioreactor. In applied mechanics and materials (Vol. 448, pp. 1675–1678), Trans Tech Publications Ltd. 448 (2014) 1675–1678.
- [55] W.H. Thomas, C.H. Gibson, Effects of small-scale turbulence on microalgae, *J. Appl. Phycol.* 2 (1990) 71–77.
- [56] X. Li, G. Li, Modeling and simulation of hydrodynamic bubble–liquid turbulent flows in bubble-column reactors, *Chem. Eng. Technol.* 39 (2016) 2380–2388.
- [57] N.C. Kommareddy, V.V. Ananthula, CFD simulation of algae production in airlift photobioreactor, *J. Hazard. Toxic Radioact. Waste* 21 (2017), 04017012.
- [58] J.C. Pires, M.C. Alvim-Ferraz, F.G. Martins, Photobioreactor design for microalgae production through computational fluid dynamics: a review, *Renew. Sust. Energ. Rev.* 79 (2017) 248–254.